Pergamon

Tetrahedron: Asymmetry, Vol. 8, No. 21, pp. 3675–3683, 1997

Printed in Great Britain
PII: S0957-4166(97)00476-X
0957-4166/97 $17.00 + 0.00

Estimation of the lipase PS (*Pseudomonas cepacia*) active site dimensions based on molecular mechanics calculations

X. Grabuleda,[a] C. Jaime*[a,*] and A. Guerrero*[b]

[a] Departament de Química, Facultat de Ciències, Universitat Autònoma de Barcelona, 08193-Bellaterra, Barcelona, Spain

[b] Departament de Química Orgànica Biològica, C.I.D. (CSIC) Jordi Girona 18-26, 08034-Barcelona, Spain

Abstract: Estimation of the active site dimensions of lipase PS (Amano) has been carried out for the first time through molecular modelling studies. The proposed model has been based on secondary alcohols, which are efficiently enantiodifferentiated by the enzyme as substrates. Some molecules which are not good substrates for the enzyme have also been used to define more precisely the limits of the active site. The model comprises three well-defined pockets: a large hydrophobic pocket of 7×6.6×4.4 Å^3 to interact with large hydrophobic substituents, a more hydrophilic pocket of *ca* 1.8×1.8×1.5 Å^3 to bind the hydroxyl group and a tunnel-shaped hydrophobic pocket (2 Å wide and 1.9 Å high) able to accomodate long side chains. The latter pocket is unique among the active site models described so far for other enzymes, which are essentially cubic in space. The model is of predictive value and accounts for the enantioselectivity shown by the enzyme in transesterification reactions of secondary alcohols. © 1997 Elsevier Science Ltd

Introduction

There has been a growing interest among organic chemists to utilize enzyme-catalyzed reactions to prepare enantiomerically pure compounds.[1–9] Lipases and esterases are the most widely employed among synthetically used enzymes since they induce high enantioselectivity, possess high activity and stability both in aqueous medium and organic solvents and can be applied to a large variety of substrates.[10–14] The desirable wide application of a specific enzyme requires knowledge of the factors which control the enantioselectivity of the recognition process by the enzyme. In this context, substrate models have been reported to determine which structures may be suitable for recognition by a specific enzyme. These models have been developed by substrate screening processes or by empirical rules.[11,13,15–21] This approach is generally limited to substrates structurally related to those from which the model has arisen. Therefore, more general models have appeared very recently to more precisely define the dimensions of the active site of the enzyme. Thus, active site models for pig liver esterase,[22,23] cyclohexanone monooxygenase (CMO),[24,25] lipase YS (*Pseudomonas fluorescens*),[26,27] and lipase AK (*Pseudomonas* sp.)[28] have been reported. For lipase PS (*Pseudomonas cepacia*) a very preliminary account on the maximum width of the hydrophobic pocket has also been reported.[29] X-ray crystallography, which provides important information on the active site of enzymes, has allowed the determination of the crystal structures of only five lipases, i.e. *Mucor miehei*,[30] human pancreatic lipase,[31] *Geotrichum candidum*,[32] *Candida rugosa*[33] and *Pseudomonas glumae*.[34] In this paper the first estimated dimensions of the active site of lipase PS, one of the most widely used enzymes for enantiodifferentiation of racemic secondary alcohols in transesterification reactions,[13,19,20] is reported by a molecular modelling approach. Our study is expected to provide further insight on the structural requirements of the active site of this enzyme in order to predict and expand the scope of new enantioselective applications of the enzyme.

* Corresponding author. Email: iqorl@cc.uab.es

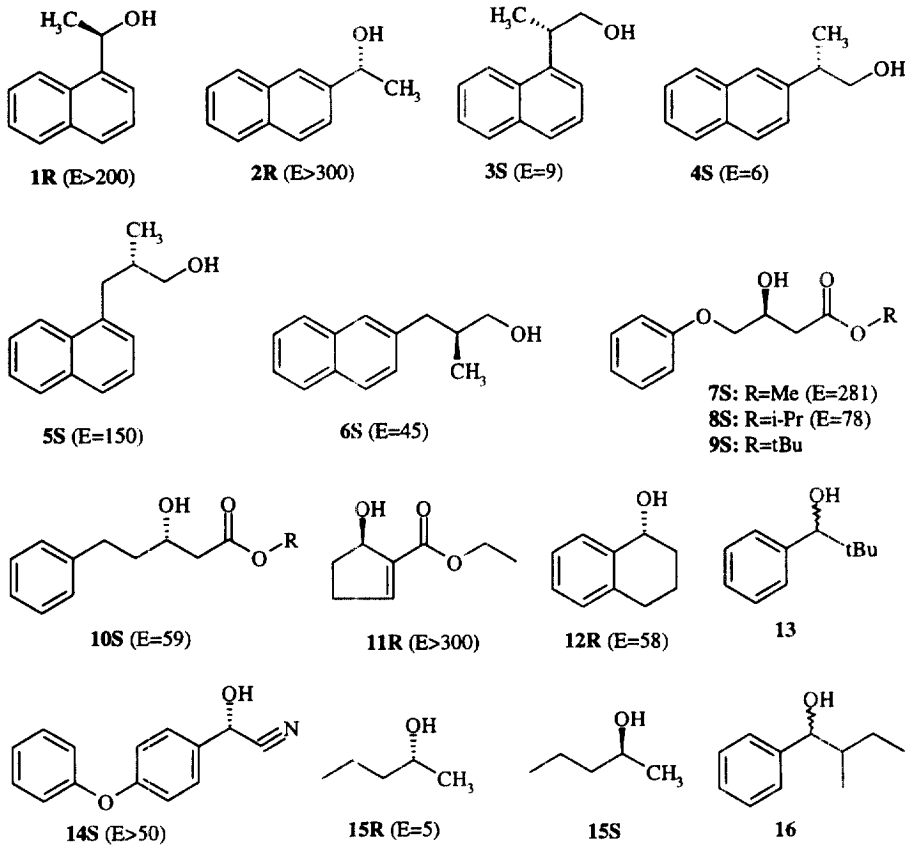

Figure 1. Structures of compounds used in this work. Numbering containing specification of the fast reactive enantiomer towards lipase PS are followed by E (enantiomeric ratio) values in parenthesis, except for compounds **15S** (not cited by Nakamura *et al.*[42]) and **9**, **13**, and **16** which are not good substrates for the enzyme.

Results and discussion

The substrates selected in this study are the following: (*R*)-1-(1′naphthyl)ethanol **1R**,[35] (*R*)-1-(2′-naphthyl)ethanol **2R**,[35] (*S*)-2-(1′-naphthyl)propanol **3S**,[36] (*S*)-2-(2′-naphthyl)propanol **4S**,[36] (*S*)-3-(1′-naphthyl)isopropanol **5S**,[36] (*S*)-3-(2′-naphthyl)isopropanol **6S**,[36] (*S*)-1-acetoxy-3-phenoxy-2-propanol **7S**,[19] (*S*)-1-isobutyryloxy-3-phenoxy-2-propanol **8S**,[19] (*S*)-3-phenoxy-1-pivaloyloxy-2-propanol **9S**,[19] (*S*)-2-hydroxy-4-phenylbutanoic acid **10S**,[37] (*R*)-2-(ethoxycarbonyl)-2-cyclopenten-1-ol **11R**,[38] (*R*)-1,2,3,4-tetrahydro-1-naphthol **12R**,[39,40] *tert*-butylphenylmethanol **13**,[40] (*S*)-cyano-4-(phenoxy)phenylmethanol **14S**,[41] (*R*)-2-pentanol **15R**,[42] (*S*)-2-pentanol **15S** and *sec*-butylphenylmethanol[40] **16**. Chirality of the reactive enantiomer towards the enzyme is also indicated in the numbering of the compound, and the E value reported is included in Figure 1.

Most of the selected compounds were good substrates for the enzyme, but poor substrates **3S**, **4S**, **15R**, **15S** and nonsubstrates **9S**, **13** and **16** were also considered to gain insight into the limitations imposed by the active site of the enzyme.

Computational studies

Computations have been carried out on a Silicon Graphics INDY computer with R4600PC processor using Still's MacroModel v.4.0 molecular modelling package.[43] MM3* was the selected force field.[44] A tandem of E. Polak and G. Ribiere conjugate gradient (PRGC)[45] and full matrix Newton Raphson

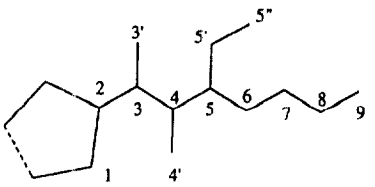

Figure 2. Generalized structure showing the numbering used throughout this work.

(FMNR) was used as a minimization algorithm allowing enough cycles to ensure the convergence in both steps.

Modelling of the active site.

All the studied substrates are conformationally flexible along their side chains. A generalized structure, showing the numbering used on all compounds of this work for the torsion angles definition, considering that the hydroxyl groups are the active centers of our target molecules, is given in Figure 2 (number 1 is given to the next atom in the clockwise direction around the ring).

A conformational analysis on molecules **1R–7S** and **10S–11R** was initially undertaken with the final aim of obtaining the global minimum energy for each structure. The number of torsion angles driven depends on the substrate, and changes from 1 to 6. The torsional energy coverage was done at increments of 15° and varying torsion angles from +180° to −180°. Structures showing the global minimum energy were further minimized without any restraint. Details on the energy minima obtained for the studied molecules in this conformational analysis are contained in Table 1. The global minima were superimposed with the aid of the SuprA and RigSA options of MacroModel. The strategic atoms chosen for this superimposition were the hydroxylic oxygen, the carbon atom supporting the hydroxyl group, and its neighbour carbon atom closer to the ring. A very diffuse cavity was obtained by using these minima, presenting a volume too large to be reasonable (largest pocket was about 5.8×7×6.9 A^3). In a second step, one of the less flexible molecules, **1R**, was taken as the model structure. It was considered as the molecule suffering the smallest geometrical changes when complexed with the enzyme, because apart from the energy minimum in Table 1 presents another conformation (1.5 kJ/mol higher in energy) which only differs in the spatial disposition of the H_L cavity but not in its dimensions. Since any molecule can be included into the active site of an enzyme in a conformation different from that showing the global minimum energy,[46] molecules **2R–7S** and **10S–12R** were superimposed on our model structure **1R** forcing the requirement of the smallest possible deviation. Molecules had to change their torsion angles adopting more energetic conformations to fulfill this requisite, increasing their energy up to about 100 kJ/mol.

Nevertheless, and to further approach the real situation of enzyme–ligand interactions, the fully superimposed structures were, thus, allowed to freely minimize their energies by changing the necessary torsion angles. Final torsion angles and energy values for these optimized well-fitting conformers are shown in brackets in Table 1. The largest energy difference between the global energy minimum calculated above and the one finally obtained is of about 16 kJ/mol for compound **10S**. If we consider that one single hydrogen bond offers a stabilization of about that amount, the differences obtained in steric energy values appeared to be very reasonable and easy to compensate by the formation of some attractive intermolecular interactions (hydrogen bonds or π–π enzyme–substrate interactions).

Figure 3 shows a stereoview image for the superimposition of molecules **2R, 5S–7S** and **10S–12R** used to define the cavity with a calculated global volume of 394.4 $Å^3$. Structures **3S** and **4S**, which presented low E values (9 and 6, respectively),[36] were used to delimit dimensions and the shape of our active site model, since the naphthalene ring is forced to adopt a conformation clearly distorted with regard to the others. Figure 4 shows a stereoview image of the volume occupied by structures **3S** and

Table 1. Dihedral angles (in degrees), and steric energies (in kJ/mol) for the minimum energy conformations of molecules **1R–7S**, **10S** and **11R** as obtained by driver calculations with the MacroModel package. In brackets are dihedral angles (in degrees), and steric energies (in kJ/mol) for conformations of molecules **1R–7S**, **10S** and **11R** which superimpose molecule **1R** better

Comp.	4-3-2-1	4′-4-3-2	5-4-3-2	6-5-4-3	7-6-5-4	8-7-6-5	9-8-7-6	5″-5′-5-6	Steric E.
1R	25.8								54.48
2R	-140.2 (40.0)								50.20 (50.38)
3S	-173.0 (-172.8)	57.7 (92.1)							68.94 (78.27)
4S	180.0 (180.0)	120.0 (120.0)							56.93 (56.93)
5S	-62.0 (-174.0)	-62.0 (-61.0)		100.8 (-78.0)					58.58 (63.36)
6S	-61.4 (-174.0)	-59.6 (-60.0)		-77.7 (106.4)					52.79 (54.80)
7S	-179.5 (180.0)		-67.2 (-179.2)	-151.2 (-174.8)	66.7 (-65.3)	-179.4 (-179.6)	179.2 (0.7)		67.91 (74.56)
10S	-177.9 (179.6)		-98.3 (116.4)	178.0 (70.1)	-60.1 (176.5)	102.4 (-94.3)		26.3 (29.4)	33.57 (49.35)
11R	180.0 (179.5)		180.0 (-179.6)	6.0 (6.1)					70.21 (70.21)

4S which exceeds the global volume of the cavity. As depicted in Figure 4, the main differences come from the aromatic rings and afford an excess volume of 58.2 Å^3. Moreover, both enantiomers of **3** and **4** show similar spatial conformation indicating a poor enantiodifferentiation process by the enzyme.

Combining the data from the superimposition of molecules **2R–7S** and **10S–12R** on **1R** as a rigid model, the active site of lipase PS is predicted to have the dimensions and shape as depicted in Figure 5. The active center should contain a large cubic hydrophobic pocket H_L of *ca* 7×6.6×4.4 Å^3, able to accommodate the aromatic rings, and a second tunnel-shaped hydrophobic pocket H_S, able to interact with long side chains such as those for compounds related to **7S**.[19] This long tunnel or hole might be 2 Å wide and 1.9 Å high and is in agreement with a proposed "long flat tube" reported by Theil and coworkers.[19] Besides these two well defined hydrophobic pockets, one smaller and more hydrophilic pocket H_H of *ca* 1.8×1.8×1.5 Å^3 appears to be also necessary to bind the hydroxyl group.

In order to validate our proposed active site model, several compounds were selected and their structures tried to fit into the model taking into account the following guidelines. First, the catalytic essential region has been considered to be located into the more hydrophilic pocket H_H, and therefore the secondary hydroxyl groups to be acylated have been placed into this region. Second, the largest hydrophobic portion of the substrate has been located into the large hydrophobic pocket H_L, while the smaller substituting group of the carbinol occupies the narrower hydrophobic pocket H_S. Under these criteria a compound is not a good substrate for the enzyme if the considered structure does not fit into the model.

Compound **8** can thus be well enantiodifferentiated by the enzyme.[19] The phenoxymethyl group of compound **8S** and the ester part of the molecule can be clearly accommodated into the H_L and H_S pockets, the isobutyryloxy group occupying the complete width of the tunnel. Following a similar rationale, compound **7** with an acetoxy group (R=Me) and other related compounds (R=long chain alkyl groups, n=1–15) could also be predicted as good substrates for the enzyme as experimentally observed.[19]

However, the pivaloyloxy derivative **9** (R=*t*-Bu) cannot fit into the H_S pocket showing that the compound is not suitable as a substrate for the enzyme. The projection on the *x*–*y* plane of the C–C

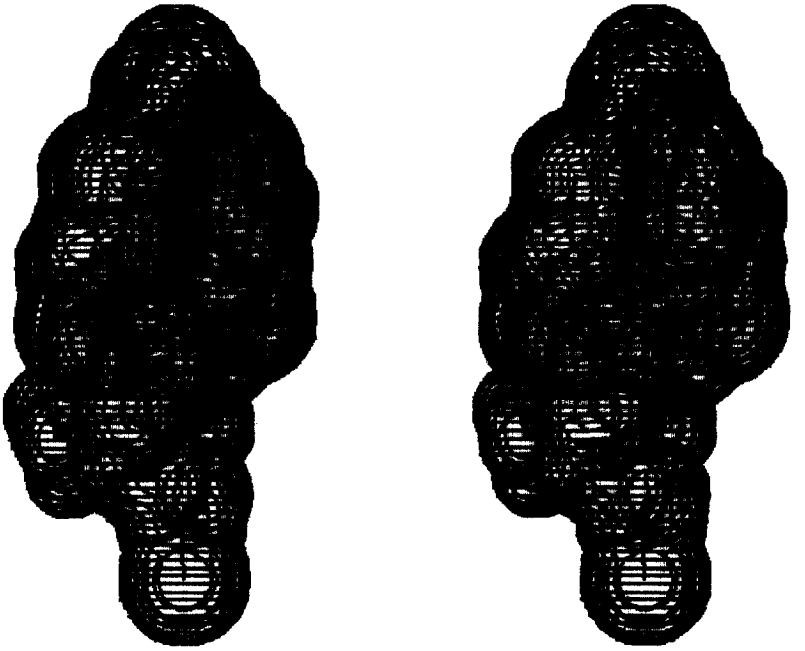

Figure 3. Stereoview of the superimpositon of molecules **2R**, **5S–7S** and **10S–12R** on **1R** as model structure and the Van der Waals volume as obtained by the MM3* calculations.

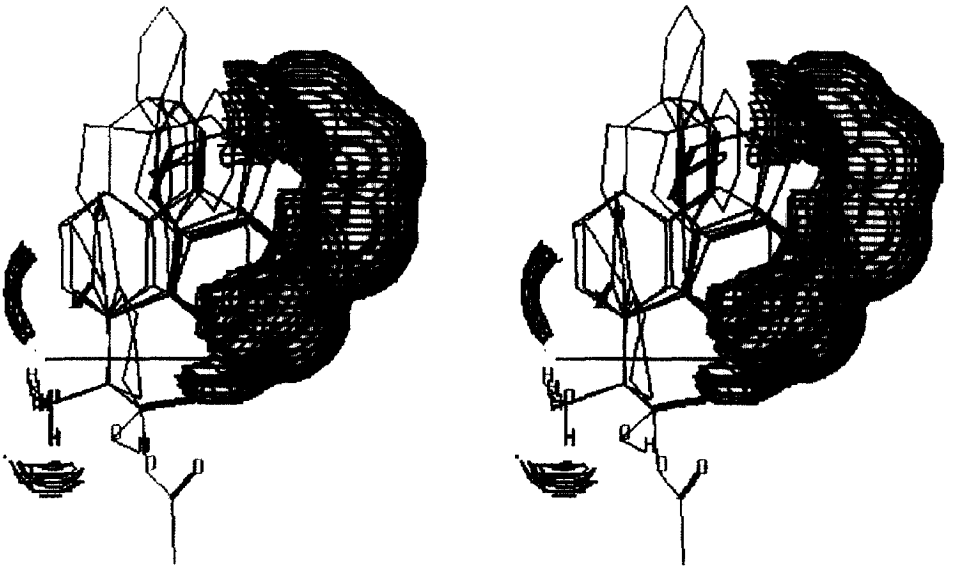

Figure 4. Stereoview of molecules **2R–7S** and **10S–12R** as model structure. Molecules **3S** and **4S** are drawn in black to better show their larger volume.

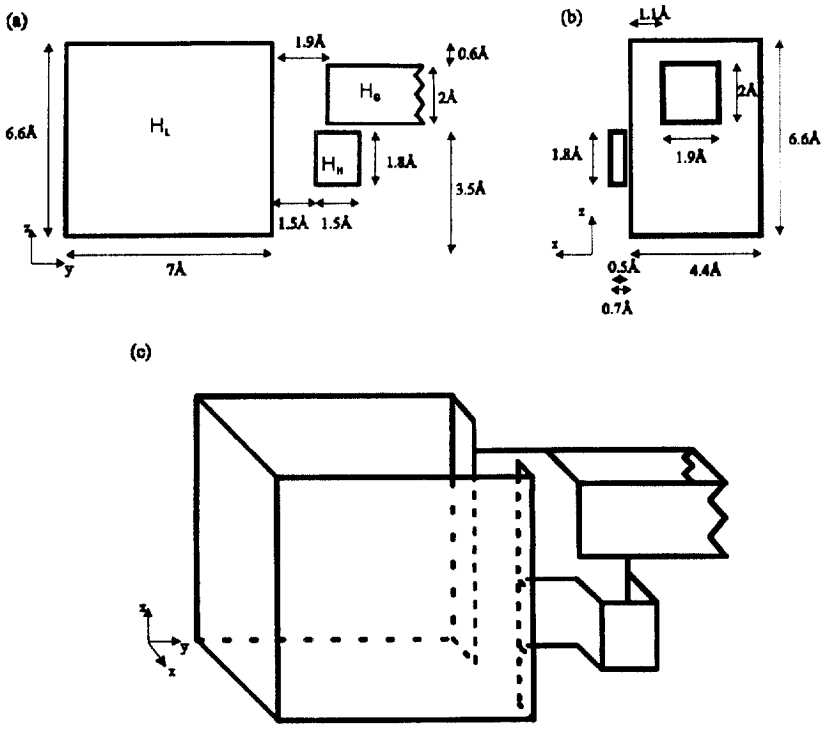

Figure 5. Dimensions and shape of the proposed active site of lipase PS. Important binding regions for substrate specificity are the large hydrophobic pocket H_L, a smaller tunnel-shaped hydrophobic pocket H_S, and a more hydrophilic cavity for the hydroxyl group H_H: (a) front perspective; (b) side perspective; (c) three dimensional representation.

bond of the methyl group which run out of the cavity limits in molecule **9S** is 0.4 Å larger than the analogous value in molecule **8S** which can be differentiated by the enzyme. Figure 6 shows, in terms of excess volume, the fragments of molecule **9S** which go out of the global cavity volume and which can be valued in 51.7 $Å^3$. In this case, the alternative binding mode, which is the basis for a reversal of stereoselectivity shown by the enzyme,[47] i.e. placing the pivaloyloxy group into H_L and the phenoxymethyl moiety into H_S, is not favored either since the latter group cannot be accommodated into the smaller pocket. The same rationale can account for the lack of recognition of compounds **13** and **16**, with a *t*-butyl and *sec*-butyl group directly joined to the carbinol, by the enzyme (no reaction after 69 h at 37°C in the presence of 2 mg of lipase PS per mmole of substrate and 10 mmole of vinyl acetate). For example, in molecule **13** the extra volume is about 45.1 $Å^3$ for enantiomer **S** and 16.4 $Å^3$ for enantiomer **R** with t-butyl being the the most important fragment which goes out. With regard to compound **14**, the phenoxyphenyl group almost fills up the large hydrophobic pocket H_L, therefore providing a high e.e. for the *S* enantiomer (E>50) (Figure 7) as experimentally found.[41] When the small molecule **15** was considered, both enantiomers easily enter into either of the two hydrophobic pockets of the model. The excess of room left by each enantiomer implies no clear preference in the binding mode in either case, and therefore no enantiodifferentiation by the enzyme could be expected (Figure 7). This has also been experimentally shown.[42]

Conclusions

In summary, and for the first time, the active site model of lipase PS has been estimated based on molecular mechanics calculations using secondary alcohols as substrates. The model comprises three well-defined pockets: two hydrophobic to accomodate the large and small hydrophobic substituents

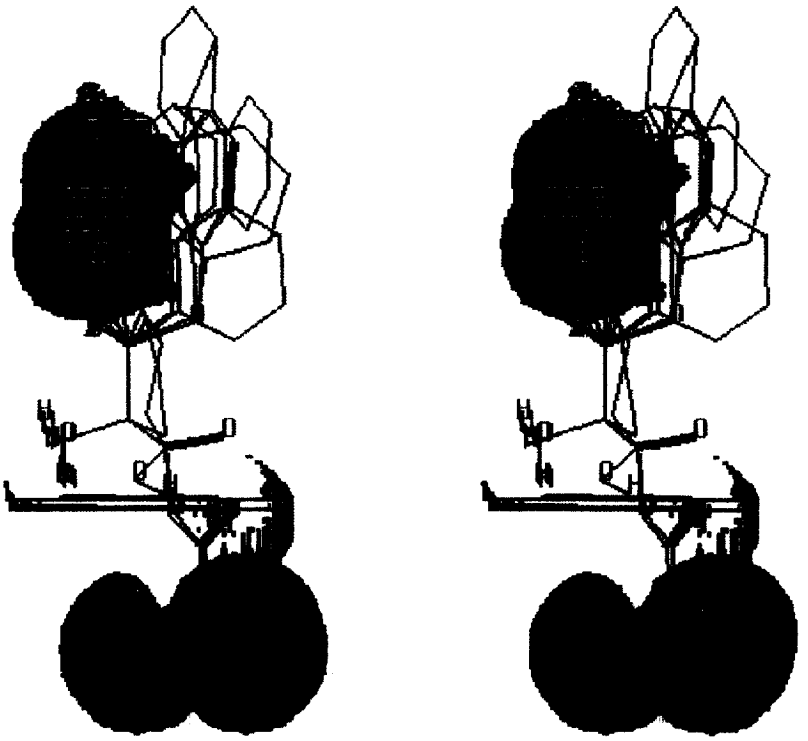

Figure 6. Stereoview of molecules **2R–7S** and **10S–12R** as model structure showing the Van der Waals volume differences. Molecule **9S** is drawn in black to better show its larger volume.

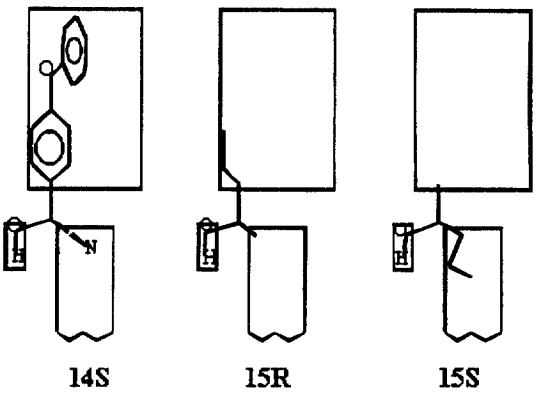

Figure 7. Top perspective views of the active site model illustrating the binding modes with the structures shown.

and a more hydrophilic tunnel-shaped pocket. The latter pocket is unique among the active site models described so far for other enzymes, which are essentially cubic in space.[22,23,26,28,48] Our model does not take into account possible modifications of the lipase PS conformations in the presence of different organic solvents, which may affect the enantioselectivity of the enzyme.[42,49] The model has predictive value for resolution of most secondary alcohols in transesterification processes by lipase PS, but it is likely that the dimensions provided herein could be refined in the near future when more data is accumulated from the literature. Experiments are in progress in our laboratory in this direction,

paying particularly attention to the so far unknown length of the tube-shaped hydrophobic pocket, unprecedented in other lipases. Also, homology modelling of lipase PS using the reported X-ray structure of *Pseudomonas glumae*[34] should also be useful to predict more precisely the active site shape of lipase PS.

Acknowledgements

Financial support from CICYT (PB 93-0158, AGF 95-0185 and PB92-0611) is gratefully acknowledged. UAB is thanked for a fellowship to one of us (X.G.).

References

1. Boland, W.; Frössl, C.; Lorenz, M. *Synthesis* **1991**, 1049.
2. Chen, C. S.; Sih, C. J. *Angew. Chem. Int. Ed. Engl.* **1989**, *28*, 695.
3. Jones, J. B. *Tetrahedron* **1986**, *42*, 3351.
4. Klibanov, A. M. *Acc. Chem. Res.* **1990**, *23*, 114.
5. Kvittingen, L. *Tetrahedron* **1994**, *50*, 8253.
6. Theil, F. *Chem. Rev.* **1995**, *95*, 2203.
7. Whitesides, G. M.; Wong, C.-H. *Angew. Chem. Int. Ed. Engl.* **1985**, *24*, 617.
8. Schoffers, E.; Golebiowski, A.; Johnson, C. R. *Tetrahedron* **1996**, *52*, 3769.
9. Mori, K. *Synlett* **1995**, 1097.
10. Roberts, S. M. *Pure Appl. Chem.* **1992**, *64*, 1933.
11. Xie, Z.-F. *Tetrahedron: Asymmetry* **1991**, *2*, 733.
12. Blanco, L.; Guibé-Jampel, E.; Rousseau, G. *Tetrahedron Lett.* **1988**, *29*, 1915.
13. Weissfloch, A. N. E.; Jazlauskas, R. J. *J. Org. Chem.* **1995**, *60*, 6959.
14. Faber, K.; Riva, S. *Synthesis* **1992**, 895.
15. Oberhauser, T.; Faber, K.; Griengl, H. *Tetrahedron* **1989**, *45*, 1679.
16. Xie, Z.-F.; Suemune, H.; Sakai, K. *J. Chem. Soc. Chem. Comm.* **1988**, 1638.
17. Kazlauskas, R. J.; Weissfloch, A. N. E.; Rappaport, A. T.; Cuccia, L. A. *J. Org. Chem.* **1991**, *56*, 2656.
18. Kim, M. J.; Cho, H. *J. Chem. Soc. Chem. Comm.* **1992**, 1411.
19. Theil, F.; Lemke, K.; Ballschuh, S.; Kunath, A.; Schick, H. *Tetrahedron: Asymmetry* **1995**, *6*, 1323.
20. Theil, F.; Weidner, J.; Ballschuh, S.; Kunath, A.; Schick, H. *J. Org. Chem.* **1994**, *59*, 388.
21. Franssen, M. C. R.; Jongejan, H.; Kooijman, H.; Spek, A. L.; Camacho Mondril, N. L. F. L.; Boavida dos Santos, P. M. A. C.; de Groot, A. *Tetrahedron: Asymmetry* **1996**, *7*, 497.
22. Toone, E. J.; Werth, M. J.; Jones, J. B. *J. Am. Chem. Soc.* **1990**, *112*, 4946.
23. Provencher, L.; Jones, J. B. *J. Org. Chem.* **1994**, *59*, 2729.
24. Ottolina, G.; Pasta, P.; Carrea, G.; Colonna, S.; Dallavalle, S.; Holland, H. L. *Tetrahedron: Asymmetry* **1995**, *6*, 1375.
25. Ottolina, G.; Carrea, G.; Colonna, S.; Rückemann, A. *Tetrahedron: Asymmetry* **1996**, *7*, 1123.
26. Naemura, K.; Fukuda, R.; Konishi, M.; Hirose, K.; Tobe, Y. *J. Chem. Soc. Perkin Trans 1* **1994**, 1253.
27. Naemura, K.; Fukuda, R.; Murata, M.; Konishi, M.; Hirose, K.; Tobe, Y. *Tetrahedron: Asymmetry* **1995**, *6*, 2385.
28. Burgess, K.; Jennings, L. D. *J. Am. Chem. Soc.* **1991**, *113*, 6129.
29. Exl, C.; Hönig, H.; Renner, G.; Rogi-Kohlenprath, R.; Seebauer, V.; Seufer-Wasserthal, P. *Tetrahedron: Asymmetry* **1992**, *3*, 1391.
30. Brady, L.; Brzozowski, A. M.; Darewenda, Z. S.; Dodson, E.; Dodson, G.; Tolley, S.; Turkenburg, J. P.; Christiansen, L.; Huge-Jensen, B.; Norskov, L.; Thim, L.; Menge, U. *Nature* **1990**, *343*, 767.
31. Winkler, F. K.; D'Arcy, A.; Hunzicker, W. *Nature* **1990**, *343*, 771.
32. Schrag, J. D.; Li, Y.; Wu, S.; Cygler, M. *Nature* **1991**, *351*, 761.

33. Cygler, M.; Grochulski, P.; Kazlauskas, R. J.; Schrag, J. D.; Bouthillier, F.; Rubin, B.; Serrequi, A. N.; Gupta, A. K. *J. Am. Chem. Soc.* **1994**, *116*, 3180.
34. Noble, M. E. M.; Cleasby, A.; Johnson, L. N.; Egmond, M. R.; Frenken, L. G. J. *FEBS Lett.* **1993**, *331*, 123.
35. Gaspar, J.; Guerrero, A. *Tetrahedron: Asymmetry* **1995**, *6*, 231.
36. Ferraboschi, P.; Casati, S.; Manzocchi, A.; Santaniello, E. *Tetrahedron: Asymmetry* **1995**, *6*, 1521.
37. Chadha, A.; Manohar, M. *Tetrahedron: Asymmetry* **1995**, *6*, 651.
38. Yamane, T.; Takahashi, M.; Ogasawara, K. *Synthesis* **1995**, 444.
39. Gutman, A. L.; Brenner, D.; Boltanski, A. *Tetrahedron: Asymmetry* **1993**, *4*, 839.
40. Chen, Zh., Bosch, M. P.; Guerrero, A., unpublished.
41. Hirohara, H.; Mitsuda, S.; Ando, E.; Komaki, R. In *Biocatalysis in Organic Syntheses;* Tramper, J., van der Plas, H. C., Linko, P., Eds.; Elsevier: Amsterdam, 1985, p. 119.
42. Nakamura, K.; Kinoshita, M.; Ohno, A. *Tetrahedron* **1995**, *51*, 8799.
43. Mohamdai, F.; Richards, N. G. J.; Guida, W. C.; Liskamp, R.; Caufield, C.; Chang, G.; Hendrickson, T.; Still, W. C. *J. Comput. Chem.* **1990**, *11*, 440.
44. Allinger, N. L. *J. Am. Chem. Soc.* **1989**, *111*, 8551.
45. Polak, E.; Ribiere, G. *Rev. Fr. Inf. Rech. Oper.* **1969**, *16*, 35.
46. Propst, C. L.; Perun, T. J. *Computer-aided Drug Design. Methods and Applications;* Marcel Dekker, Inc.: New York, 1989.
47. Jencks, W. P. *Adv. Enzymol.* **1975**, *43*, 219.
48. Naemura, K.; Murata, M.; Tanaka, R.; Yano, M.; Hirose, K.; Tobe, Y. *Tetrahedron: Asymmetry* **1996**, *7*, 1581.
49. Nakamura, K.; Takebe, Y.; Kitayama T.; Ohno, A. *Tetrahedron Lett.* **1991**, *32*, 4941.

(*Received in UK 19 September 1997*)